

Improved Algorithm for Time-Domain Electromagnetic Field Calculation at Points outside the TLM Workspace

Nebojša Dončov and Bratislav Milovanović

Abstract – In this paper, an algorithm for electromagnetic field calculation in the time-domain at points outside the defined TLM numerical workspace is presented. This algorithm is based on integration over Huygens surface surrounding all electromagnetic structures within the workspace. As this integration involves a significant amount of computation, a reduction of the integration frequency is suggested to improve the algorithm efficiency. This improvement incurs the cost of extra storage but has an advantage that this cost is fixed and does not increase with the number of output points. Accuracy and efficiency of the improved algorithm are illustrated on the appropriate example.

Keywords – EMC, TLM, Huygens surface, output outside workspace, integration frequency

I. INTRODUCTION

Electromagnetic compatibility (EMC) is the branch of science and engineering concerned with the design and operation of equipment in a manner which makes them immune to certain amounts of electromagnetic (EM) interference, keeping, at the same time, equipment-generated interference within specific limits [1]. The scope of EMC is thus very wide as it encompasses virtually all equipment powered by electrical supplies. In recent years, the rapid increase in the use of radio communications, digital systems, fast processors and the introduction of new design practices have brought EMC to the forefront of advanced design.

How practical modern systems exceed in complexity anything that can be solved analytically or using approximate techniques, numerical computer-based models are the only alternative to study trends in EMC design and to understand the behaviour of systems. Differential numerical techniques in the time-domain, such as Finite-Difference Time-Domain (FD-TD) [2] and Transmission-Line Matrix (TLM) [3], are well established for solving a number of EMC problems over a wide frequency range. These methods, due to their characteristics and the development of powerful computer stations, offer a significant extension of the range of EMC problems that can be tackled.

However, there are still numerous practical EMC problems, where these techniques, even with the use of powerful computer stations are incapable to allow for their fast and correct modelling. One area of inefficient EMC

numerical simulation represents equipment containing geometrically small but electrically important features (e.g. thin wires, slots, air-vents). For their description, extremely fine mesh is required which can result in a prohibitively large number of cells and large number of time-steps. In recent years, enhancements to TLM technique in the form of so called sub-cell or compact models have been developed to allow for an efficient simulation of these structures [4-6]. Prediction of level of interference generated by such equipment, as one of the key concerns in EMC design, is another area where numerical techniques struggle to allow calculation of EM field response at points located at distances exceeding the dimensions of radiating EM structures, by one order of magnitude or more. Again, large number of cells is required to cover that distance between equipment and outputs which leads to time consuming and inefficient EMC simulation even with the use of developed compact models.

The algorithm for efficient EM field calculation at points located at large distances from the radiating EM structures, without defining discrete numerical mesh up to these points, has been developed and verified in [7]. It was based on Love's equivalence principle [8,9] and required definition of so-called Huygens closed surface within the workspace surrounding all EM structures of analyzed EMC problem. However, integration over the Huygens surface at every time-step, to allow calculation of the time-domain EM field at points outside the numerical workspace, involved a significant amount of computation. The computational burden for a single output point proved acceptable but it can be easily made unacceptable by specifying many output points. Therefore, in this paper it is suggested to reduce the integration frequency to once every time-sample which will incur the extra memory storage but this cost does not increase with the number of output points. Improved algorithm is again implemented in TLM method and verified on the appropriate example. Compared to the conventional simulation, huge saving in simulation run-time can be achieved and maintained with the increase of output points.

II. LOVE'S EQUIVALENCE PRINCIPLE

The surface equivalence theorem is a principle by which actual sources, represented electrically by current densities J_1 and M_1 , are replaced by equivalent sources J_s and M_s (Fig.1). The fictitious sources are said to be equivalent within a volume V_2 , because they produce within that volume the same fields (E_1 and H_1) as the actual sources. According to this principle, the fields outside an imaginary closed surface S , i.e. in volume V_2 , are obtained by placing, over the closed so-called Huygens surface, suitable electric and magnetic

Nebojša Dončov and Bratislav Milovanović are with the Faculty of Electronic Engineering, Aleksandra Medvedeva 14, 18000 Niš, Serbia and Montenegro, E-mail: [doncov, bata]@elfak.ni.ac.yu

current densities that satisfy the boundary conditions. These equivalent current densities are given by Eqs.(1) and (2).

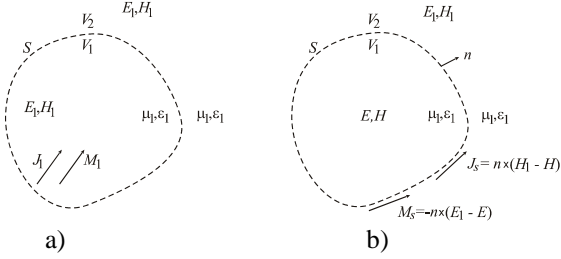


Fig.1 a) Actual and b) equivalent problem models

$$J_s = n \times (H_1 - H) \quad (1)$$

$$M_s = -n \times (E_1 - E) \quad (2)$$

The current densities are then selected so that the fields inside the closed surface (volume V_1), which is not the region of interest, are zero and outside the closed surface (volume V_2) are equal to the radiation produced by the actual sources:

$$J_s = n \times (H_1 - H)|_{H=0} = n \times H_1 \quad (3)$$

$$M_s = -n \times (E_1 - E)|_{E=0} = -n \times E_1 \quad (4)$$

Thus, this technique can be used to obtain the fields radiated outside a closed surface by sources enclosed within it. The formulation is exact but requires integration over the closed surface.

Since the current densities J_s and M_s radiate in an unbounded medium that is, have the medium (μ_1, ϵ_1) everywhere, they can be used in conjunction with the Eqs.(5) and (6) to find the fields everywhere:

$$E_1 = -j \frac{1}{\omega \mu_1 \epsilon_1} \nabla(\nabla \cdot A) - j\omega A - \frac{1}{\epsilon_1} \nabla \times F \quad (5)$$

$$H_1 = -j \frac{1}{\omega \mu_1 \epsilon_1} \nabla(\nabla \cdot F) - j\omega F + \frac{1}{\mu_1} \nabla \times A \quad (6)$$

where A and F are vector magnetic and electric potential, respectively, that can be expressed through electric and magnetic surface currents as [8]:

$$A = \frac{\mu_1}{4\pi} \int_S J_s \frac{e^{-jkR}}{R} dS', \quad F = \frac{\epsilon_1}{4\pi} \int_S M_s \frac{e^{-jkR}}{R} dS' \quad (7)$$

III. NEAR-TO-NEAR TRANSFORM ALGORITHM

The contribution of an elemental patch of the Huygens surface to EM field at a point removed from it by the vector R can be found in the time-domain from Eqs.(5-7) as:

$$\Delta E(t + R/c) = \frac{\Delta S}{4\pi R \cdot R} (\Delta E_{rad}(t) + \Delta E_{ind}(t) + \Delta E_{stat}(t)) \quad (8)$$

$$\Delta H(t + R/c) = \frac{\Delta S}{4\pi R \cdot R} (\Delta H_{rad}(t) + \Delta H_{ind}(t) + \Delta H_{stat}(t)) \quad (9)$$

where ΔS is the area of the elemental patch determined by TLM node. As it can be seen the signal from each surface patch consists of a differential radiation term (ΔE_{rad} and ΔH_{rad}), a direct induction term (ΔE_{ind} and ΔH_{ind}) and an integral static field term (ΔE_{stat} and ΔH_{stat}) that can be expressed in rectangular coordinate system as:

$$\Delta E_{rad}(t) = \frac{|R|}{c} \frac{d}{dt} (Z_0((J_s \cdot R_{ort}) \cdot R_{ort} - J_s) - M_s \times R_{ort}) \quad (10)$$

$$\Delta E_{ind}(t) = Z_0(3(J_s \cdot R_{ort}) \cdot R_{ort} - J_s) - M_s \times R_{ort} \quad (11)$$

$$\Delta E_{stat}(t) = \frac{c}{|R|} \int Z_0(3(J_s \cdot R_{ort}) \cdot R_{ort} - J_s) dt \quad (12)$$

$$\Delta H_{rad}(t) = \frac{|R|}{c} \frac{d}{dt} (Y_0((M_s \cdot R_{ort}) \cdot R_{ort} - M_s) + J_s \times R_{ort}) \quad (13)$$

$$\Delta H_{ind}(t) = Y_0(3(M_s \cdot R_{ort}) \cdot R_{ort} - M_s) + J_s \times R_{ort} \quad (14)$$

$$\Delta H_{stat}(t) = \frac{c}{R} \int Y_0(3(M_s \cdot R_{ort}) \cdot R_{ort} - M_s) dt \quad (15)$$

where Z_0 is an intrinsic impedance of free space ($Y_0 = 1/Z_0$), R_{ort} is unit vector ($R_{ort} = R/|R|$) and J_s and M_s are the equivalent electric and magnetic current densities, respectively.

The time delay R/c in the near-to-near transform is introduced by means of a conveyor belt shown in Fig.2. Each output point is at the delivery end of its own conveyor which carries a time-domain signal towards it at the speed of light c . In order to introduce a delay R/c into a signal, the signal is dropped once every time-step Δt onto the conveyor at the distance R upstream of the output point.

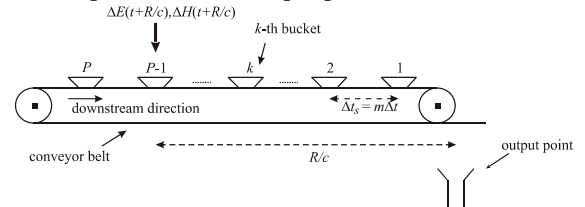


Fig.2 Conveyor belt for one output point

The conveyors are not continuous but consist of buckets spaced one time-sample, Δt_s , apart. Time-sample depends on highest frequency of interest for EM response analysis and in general can be expressed as integer number, m , of used time-step in TLM simulation, Δt ($\Delta t_s = m\Delta t$). If a signal is dropped onto the conveyor belt at time, $i\Delta t$, ($i=1,2,\dots,I_{max}$, where I_{max} is maximum number of iteration of simulation in the time-domain) when a bucket is not passing the loading point in question, then the signal falls between buckets and is lost. The conveyor belt (buckets on it) advances with time-step Δt towards output point (downstream direction).

The time delay R/c is introduced in the way that signal corresponding to the appropriate elemental patch of Huygens surface at distance R from the output point is dropped onto appropriate place at conveyor belt ($\Delta E(t+R/c)$ and $\Delta H(t+R/c)$, given by Eqs.(8-15)). The total length of a conveyor is determined by the maximum required delay, i.e. by the distance between the output point and the most remote patch of the Huygens surface and it can be calculated as:

$$P_{max} = 1 + \text{int}(R_{max} / c / \Delta t) \quad (16)$$

IV. IMPROVING THE COMPUTATIONAL EFFICIENCY

Because the integration over the Huygens surface involves a significant amount of computation, it may be worthwhile attempting to reduce the integration frequency from once

every time-step to once every time-sample. Even if the computational burden for a single output point proves acceptable, it can be easily made unacceptable by specifying many output points. The integration frequency may be reduced in a variety of ways. The approach described in this paper incurs the cost of extra storage, but has the advantage that this cost is fixed and does not increase with the number of output points.

At first, an additional conveyor belt is created for each elemental patch of the Huygens surface while keeping conveyor belt per output point as a main belt. These per-patch conveyor belts are very short, just one time-sample plus one time-step long, and have a bucket at every time-step. Each per-patch conveyor belt carries the equivalent surface currents J_s and M_s away from the patch, and it is therefore four real numbers wide.

Per-Time-Sample integration is performed as follows. For simplicity, assume that the integration is performed at those time-steps when a bucket of a main conveyor belt is level with its output point. At these time-steps there will be no buckets at any loading point corresponding to a fractional time-sample delay. In these circumstances, the delay is achieved by picking surface currents off the per-patch conveyor a distance downstream of the patch corresponding to the fractional part of the delay, doing necessary arithmetic, and then dropping the resulting values onto the main conveyor at a point corresponding to the integral part of the delay (where we have presupposed there to be a bucket present).

a) Differential radiation term

For the differential term, instead of dropping an up-down pulse onto the main conveyor belt, as suggested in [7], an up-down pulse is picked off the per-patch conveyor belt, and the resulting radiation term dropped straight into a single bucket of the main conveyor. When the desired delay n is not an exact half-integral number of time-steps, the same weightings are used as described in [7]:

$$\text{drop}[N-1] = (N+1/2-n)v(t) / \Delta t$$

$$\text{drop}[N] = 2(n-N)v(t) / \Delta t$$

$$\text{drop}[N+1] = (N-1/2-n)v(t) / \Delta t$$

where $N = \text{nint}(n)$ is the nearest integer value.

The extra time-step allowed in the length of the per-patch conveyors simplifies the case of integral and near-integral time-sample delays. Without the extra length, it would be necessary to treat these cases specially. This would involve transferring one term from one end of the per-patch line to one bucket on the main conveyor belt and a second term from the other end of the per-patch line to the adjacent bucket on the main conveyor belt doubling the necessary computation.

b) Direct term

The value for the direct induction term is simply dropped, instead of main conveyor belt, onto the per-patch conveyor belt at the desired point. Again, for fractional time-steps, the drop weightings described in [7] are now used as pickup-weightings from the per-patch conveyor:

$$\text{drop}[N1] = (N2-n)v(t)$$

$$\text{drop}[N2] = (n-N1)v(t)$$

where $N1$ and $N2$ are consecutive integers bracketing n .

c) Integral term

The main part of the integration is still performed on the main conveyor belt. It would be very inefficient to integrate surface currents from an individual patch, because of the presence of a D.C. field the integral would ramp up forever. The fractional-time-sample part of the integral is performed by picking up all values of the per-patch conveyor downstream of the desired fractional-delay point (excluding the extra time-step). The resulting term is dropped into the bucket of the main conveyor corresponding to the integral part of the delay. All buckets upstream from this one get the static field term resulting from the sum of all the values on the per-patch conveyor (whether upstream or downstream of the fractional pickup point, but excluding the extra time-step).

For fractional time-steps, the drop weightings specified in [7] is used as a pickup weighting:

$$\text{drop}[N] = (N+1/2-n)v(t)\Delta t$$

V. NUMERICAL ANALYSIS

The accuracy and efficiency of improved algorithm for calculating the time-domain EM field at points outside the TLM workspace are verified on the realistic EMC example in the form of rectangular shielding enclosure (Fig.3a). The enclosure was constructed of six pieces of $t=0.635$ cm thick aluminum with conductivity $\sigma=3.54e7$ S/m. The inside dimensions of the enclosure were $a=50$ cm, $b=20$ cm and $c=40$ cm. One of the enclosure walls in yz plane contains the square aperture array (Fig.3b). The aperture size was $l=1$ cm, with an edge-to-edge space $p=0.5$ cm. The number of apertures was 252.

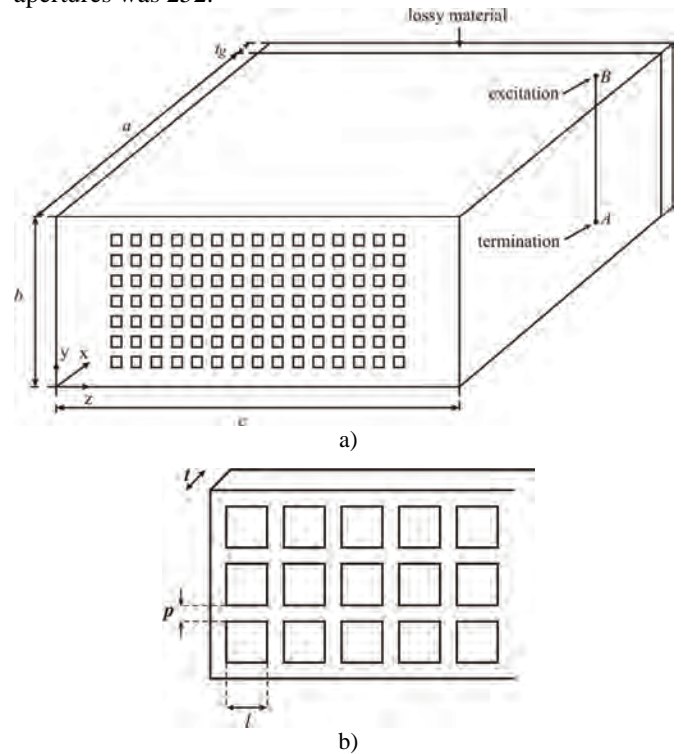


Fig.3. a) Rectangular test enclosure with air-vent on front face, b) air-vent layout

The model was excited by a long-wire feed at the back of the box which was modelled by a simple voltage source $V=1$ mV with 50 Ohm resistance incorporated into a single cell at the feed point B (43 cm, 20 cm, 33 cm). The excitation had the center conductor of the probe extended to span the width of the cavity with a 0.16 cm diameter and terminated on the opposite cavity wall with termination of 47 Ohm at point A (43 cm, 0, 33 cm). In order to reduce Q-factor of enclosure, which can be extremely high for unloaded enclosure, lossy material of conductivity $\sigma=2.27\text{S/m}$ and thickness $t_g=1$ cm was used. The resistors were modelled as lumped elements. Compact wire [4] and air-vent model [6] were used to model wire conductor and array of square apertures, respectively, in order to avoid the need of TLM mesh with extremely high resolution. The choice of geometry, excitation and output was governed by experimental arrangements used in [10].

Huygens virtual surface, completely surrounding the TLM model of the enclosure, is located at the distance of one TLM node from the enclosure. The external boundaries of TLM mesh are placed around the enclosure at the distance greater than 30% of the largest dimension of the enclosure, which is still far away from the required output point. The results for far zone electric field at 3 m away from the face of enclosure containing air-vent, obtained by using the improved algorithm, are compared with the experimental results [10] and shown in Fig.4. An excellent agreement between these two results can be observed except at higher frequencies, probably due to neglecting the frequency dependant characteristics of the lossy material at the back of the box. In addition huge saving in the computer resources, compared to conventional TLM, is achieved with accuracy acceptable for most EMC applications.

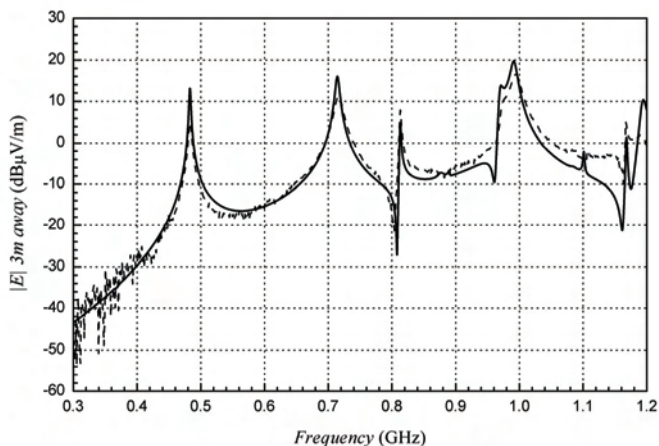


Fig.4 Radiated electric field at 3 m away from the enclosure: a) measurements (dotted line), b) improved algorithm (solid line)

VI. CONCLUSION

This paper describes an improved algorithm for calculating the time-domain EM field at points outside the TLM workspace. It is primarily indented for EMC applications. The new scheme is based again on integration over a Huygens surface within the defined workspace using the calculated equivalent electric and magnetic surface currents. However, integration frequency is now reduced from

once every time-step as suggested previously to once every time-sample in order to maintain efficiency of proposed algorithm with the number of output points. The effect of time delay in signal propagation from elemental patches of Huygens surface to output points is realized through main conveyor belt per output point and additional belts per elemental patch of Huygens surface. The scheme is general and it can be implemented into other differential numerical techniques in the time-domain such as FD-TD method. The efficiency of this approach is illustrated on the appropriate examples.

If the number of time-steps per time-sample is high, then an intermediate sampling frequency must be used on the per-patch conveyor belts to avoid excessive memory usage. There need not be a whole number of intermediate time-samples per final time-sample. However, the transfer of the static field terms from the per-patch conveyor belt to the main conveyor belt must take into account what fraction of the final intermediate time-sample must be transferred to make up a complete final time-sample. This modification to allow efficient memory allocation, in the case of high time-sample, will be presented in future papers.

REFERENCES

- [1] C. Christopoulos, *Principles and Techniques of Electromagnetic Compatibility*, CRC Press, 2000.
- [2] C. Christopoulos, *The Transmission-Line Modelling Method*, Series on Electromagnetic Wave Theory, IEEE/ OUP Press, 1995.
- [3] K.S. Kunz, R.J. Luebbers, *The Finite Difference Time Domain for Electromagnetics*, CRC Press, 1993.
- [4] A.J. Wlodarczyk, V. Trenkić, R. Scaramuzza, "A Fully Integrated Multiconductor Model for TLM", *IEEE Transactions on Microwave Theory and Techniques*, Vol.46, No.12, 1998, pp.2431-2437.
- [5] V. Trenkić, R. Scaramuzza, "Modelling of Arbitrary Slot Structures using Transmission Line Matrix (TLM) Method", *Proceedings of International Zurich Symposium on Electromagnetic Compatibility*, Zurich, Switzerland, 2001, pp.393-396.
- [6] N. Dončov, A.J. Wlodarczyk, V. Trenkić, R. Scaramuzza, "Compact TLM Model for Air-vents", *Electronics Letters*, Vol.38, No.16, 2002, pp.887-889.
- [7] N. Dončov, B.Milovanović, "Electromagnetic Field Calculation in the Time-Domain at Points outside the TLM Workspace", *Proceedings of 41st ICEST Conference*, Sofia, Bulgaria, 2006, pp.37-40.
- [8] E.C. Jordan, K.G. Balmain, *Electromagnetic Waves and Radiating Systems*, Prentice-Hall Inc., 1968.
- [9] C.A. Balanis, *Advanced Engineering Electromagnetics*, John Wiley & Sons, New York, 1989.
- [10] M.Li, J.Nuebel, J.L.Drewniak, R.E. DuBroff, T.H. Hubing and T.P.Van Doren, "EMI from Airflow Aperture Arrays in Shielding Enclosures – Experiments, FDTD, and MoM Modelling", *IEEE Transactions on Electromagnetic Compatibility*, Vol.42, No.3, pp.265-275, 2000.